



J. Serb. Chem. Soc. 81 (7) 777–787 (2016)
JSCS–4885

Raman study of the interactions between highly ordered pyrolytic graphite (HOPG) and polyoxometalates: The effects of acid concentration

BOJAN A. VIDOESKI¹, SVETLANA P. JOVANOVIĆ^{2*}, IVANKA D. HOLCLAJTNER-ANTUNOVIĆ¹, DANICA V. BAJUK-BOGDANOVIĆ¹, MILICA D. BUDIMIR², ZORAN M. MARKOVIĆ^{2,3} and BILJANA M. TODOROVIĆ MARKOVIĆ²

¹Faculty of Physical Chemistry, P. O. Box 47, University of Belgrade, 11158 Belgrade, Serbia; ²Vinča Institute of Nuclear Sciences, P. O. Box 522, University of Belgrade, 11001 Belgrade, Serbia; ³Polymer Institute Slovak Academy of Sciences, Dubravská Cesta 9, Bratislava, Slovakia

(Received 1 March, accepted 4 April 2016)

Abstract: Heteropoly acids (HPAs) have found wide applications, such as in catalysis, energy conversion and storage, analytical chemistry, clinical medicine, materials science and others, but their use is limited due to their low surface area and high solubility in water. One of the possible ways to overcome these obstacles is to use height specific surface area supports for HPAs, such as carbon nanomaterials. Raman spectroscopy was applied for a studying the interaction between HPAs and highly ordered pyrolytic graphite (HOPG) as a model of a support. HOPG was exposed to two different HPAs: 12-tungstophosphoric acid and 12-molybdophosphoric acid, at different concentrations. It was noticed that 12-molybdophosphoric acid had stronger effects on the HOPG structure causing a weak doping and an increase of structural disorder. It was supposed that HOPG interacts with especially external oxygen atoms of 12-molybdophosphoric acid. Atomic force microscopy showed that the surface roughness of HOPG treated with 12-molybdophosphoric acid increases with increasing acid concentration, while in the case of HOPG exposed to 12-tungstophosphoric acid, the surface roughness concentration independent. The growth trend in the measured surface roughness (*RMS*) was in the agreement with the changes in the intensity ratio I_D/I_G obtained from the Raman spectra of the HOPG samples treated with 12-molybdophosphoric acid.

Keywords: heteropoly acids; graphite; Raman spectroscopy; atomic force microscopy.

* Corresponding author. E-mail: svetlanajovanovic@vinca.rs
doi: 10.2298/JSC160301055V

INTRODUCTION

Polyoxometalates (POMs) represent a large class of metal oxygen clusters consisting of d-block transition metals and oxygen atoms. POMs with a Keggin structure, such as 12-tungstophosphoric acid ($\text{H}_3\text{PW}_{12}\text{O}_{40}$, WPA) and 12-molybdophosphoric acid ($\text{H}_3\text{PMo}_{12}\text{O}_{40}$, MoPA), also known as heteropoly acids (HPAs), which consist of a tetrahedral PO_4 unit surrounded by 12 MO_6 octahedral units (Fig. 1).^{1,2} Due to their strong Brønsted acidity and multiple redox properties,^{3,4} they have found application as catalysts, superionic proton conductors, sensors, sorbents, analytical reagents and many others.^{5–10} However, due to their low surface area and high solubility in water and polar solvents, their application, especially as catalysts, is restricted. These drawbacks could be overcome by supporting POMs on insoluble substrates, such as amorphous and mesoporous silica, titania, alumina or recently, carbon nanomaterials.^{11–13}

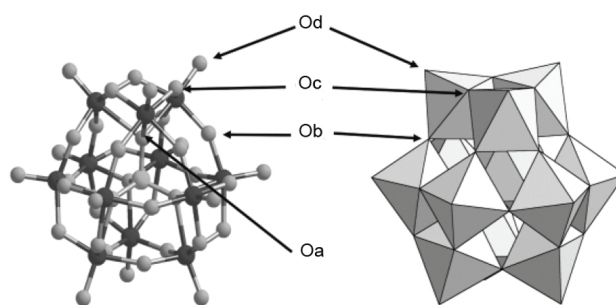


Fig. 1. Polyhedral representation of the molecular Keggin-structure POM.

Highly ordered pyrolytic graphite (HOPG) is a pure and ordered form of synthetic graphite. The crystal structure of HOPG consists of stacked parallel layers of two-dimensional, one-atom thick form of carbon, so-called graphene. The sp^2 hybrid orbitals of the C atoms are connected with two other sp^2 orbitals in graphite. This leads to the formation of a hexagonal planar structure of C atoms. In this structure, one electron is left on each carbon atom. Thus, these electrons create a delocalized π -electron cloud and give good metallic electrical conductivity within the plane direction. However, perpendicular to this plane, graphite acts as an insulator. Considering their atomically flat surface and metallic conductivity, HOPG is an ideal substrate for scanning probe microscopy. HOPG has been also studied for application as an electrode support for electro-deposition, nanostructured interfaces for biosensing and model of nanoparticle electrocatalysts.^{14–16}

In spite of the fact that there are studies concerning HPAs deposited on HOPG,^{17–26} the type of interaction between these two materials has not been investigated and understood. In the present study, two different HPAs supported

by HOPG were prepared. Raman spectroscopy and atomic force microscopy (AFM) were used to study the interactions of HOPG with WPA and/or MoPA. These methods allowed the interactions and structural changes in HOPG caused by WPA and MoPA solutions to be investigated. The effects of different solution concentrations of the HPAs were also analyzed.

EXPERIMENTAL

Materials

WPA was prepared by a previously described method²⁷ and recrystallized prior to use, while MoPA was purchased from Merck, Darmstadt, Germany. In order to obtain stable acid hexahydrates, the WPA and MoPA were heated up to 80 and 60 °C, respectively.

HOPG was obtained by heat treatment of pyrolytic carbon at 3500 °C under high pressure (Materials Science Laboratory, Vinča Institute of Nuclear Sciences, Serbia).

Four nearly uniform pieces of HOPG (20 mg) were prepared and mixed with water–methanol mixtures (1:1) of WPA and MoPA.²⁸ The concentrations of the WPA solutions were 3.4×10^{-4} and 3.4×10^{-3} mol dm⁻³ and for MoPA 5.2×10^{-4} and 5.2×10^{-3} mol dm⁻³. After mixing HOPG pieces with HPAs solutions, 1 vol. % of ethylene glycol was added to assure diffusion of HPAs on the surface of HOPG. The samples were stirred for 24 h at room temperature, then washed with deionized water and dried in air. The samples prepared with the lower concentration of HPAs are named as HOPG–HPA (1:1), while those mixed with the higher concentration of HPAs are designated as HOPG–HPA (1:10). In all cases, the ratio is expressed as mass of HOPG to mass of HPAs in the initial reaction mixture.

Additionally, the effect of short-term exposure of HPAs on the HOPG structure was studied. Thus, 1 mL of 1.0×10^{-1} mol dm⁻³ of WPA water solution was deposited on HOPG (30 mg). The sample was left at room temperature in an air atmosphere for 30 min and then dried in an argon stream. In the further text, this sample is referred to as HOPG–WPA (1:10)-C, where C stands for concentrated solutions.

Furthermore, long-term exposure to the high concentration of MoPA on HOPG was studied. HOPG (39 mg) was mixed with 387 mg of MoPA in 2 mL of water–methanol mixture (1:1) with 1 vol. % of ethylene glycol. After 24 h of stirring at room temperature, the HOPG was washed with deionized water (2 mL) and dried. The sample was named HOPG–MoPA (1:10)-C. In order to investigate fully the influence of an excess of MoPA on the characteristics of the obtained composite, this sample was left in a water–methanol solution for about 15 min followed by drying in air at the room temperature. This washed sample was labeled as HOPG–MoPA (1:10)-C_w. For an easier review, all samples with their labels in the text are presented in Table I.

TABLE I. Summarized samples with their designated labels

Type of sample	Sample name	Concentration of HPA, mol dm ⁻³
HOPG–WPA	HOPG–WPA (1:1)	3.4×10^{-4}
	HOPG–WPA (1:10)	3.4×10^{-3}
	HOPG–WPA (1:10)-C	0.10
HOPG–MoPA	HOPG–MoPA (1:1)	5.2×10^{-4}
	HOPG–MoPA (1:10)	5.2×10^{-3}
	HOPG–MoPA (1:10)-C	0.10
	HOPG–MoPA (1:10)-C _w	0.10

Equipment

All Raman spectra were collected by a DXR Raman microscope (Thermo Scientific) equipped with a motorized *X–Y* stage and a CCD detector. The wavelength of the excitation source was 532 nm with a laser power of 5 and 10 mW. The scattered light was collected through an Olympus microscope with infinity corrected confocal optics, a 50 μm pinhole aperture and a 50 \times standard working distance objective. The spectral resolution was 1 cm^{-1} . Thermo Scientific OMNIC software was used for spectra collection and manipulation.

AFM measurements were performed using a Quesant microscope operated in the tapping mode in air at the room temperature.²⁹ We used An AFM Q-WM300 probe, a rotated, monolithic silicon probe for non-contact high frequency applications, was used. Standard silicon tips (Nano and More GmbH., Wetzlar, Germany) were used, with a force constant of 40 N m^{-1} . Gwyddion software was used for detailed surface analysis of the HOPG samples and for surface roughness calculations.³⁰

RESULTS AND DISCUSSION

Raman spectroscopy is an important and widely used method for the characterization of both carbon materials and POMs since it is very sensitive to structure and bonding within molecules. The Raman spectra of HOPG shows two prominent bands and, occasionally, a third one.³¹ The first prominent band is the so-called G band. It corresponds to the in-plane (E_{2g}) vibration mode of sp^2 hybridized carbon atoms and is located at around 1580 cm^{-1} . In Raman spectra, the other band can also appear. This band is called the D-band and it corresponds to the in-plane (A_{1g}) zone edge mode. The D-band results from defects in the sp^2 carbon lattice and is expected at around 1350 cm^{-1} . By observing the intensity ratio of the D and G bands (I_D/I_G), it is possible to determine the presence and level of defects in the sample. The third band is the 2D band, historically designated as G' , the second order band of the D band and it can be expected at about 2700 cm^{-1} . Furthermore, the number of graphene layers can be calculated from the intensity ratio of 2D and G bands (I_{2D}/I_G).³²

Due to its extreme sensitivity to structural changes, Raman spectroscopy has been used as one of the main characterization method when analyzing POMs.

The Raman spectra of both WPA and MoPA contain high intensity bands in the interval 1050–800 cm^{-1} . The characteristic prominent bands of the Keggin anion are assigned to the stretching vibrations $\nu_s(\text{M}=\text{O}_d)$ at about 1010 and 995 cm^{-1} , a mix of the stretching vibrations $\nu_{as}(\text{M}=\text{O}_d)$ and $\nu_s(\text{P}-\text{O}_a)$ at about 995 and 980 cm^{-1} and $\nu_s(\text{M}-\text{O}_b-\text{M})$ stretching vibrations at about 925 and 900 cm^{-1} , respectively, for WPA and MoPA.³³

Raman spectra of pristine HOPG and HOPG–WPA samples with different mass ratio are presented in Fig. S-1 of the Supplementary material to this paper. Three prominent bands were observed: at 1350, 1581 and 2700 cm^{-1} . All these bands stem from HOPG. On the contrary, no bands could be observed in the interval 1050–800 cm^{-1} . The lack of WPA bands can be assign to the low concentration sensitivity of Raman spectroscopy.

The positions of the corresponding bands are presented in Table II. These results show that there were no changes in the positions or shapes of the bands. Therefore, there was no charge transfer between HOPG and WPA. However, the I_D/I_G ratio of the HOPG–WPA samples (0.08 and 0.05 for HOPG–WPA (1:1) and HOPG–WPA (1:10), respectively) differed from I_D/I_G ratio of pristine HOPG (0.06). The observed changes of I_D/I_G were in dependence on the fraction of WPA in the samples – the samples with the lower fraction of WPA indicate that the intensity ratio I_D/I_G increased, while the samples with the higher amount of WPA showed that the ratio decreased.

TABLE II. Positions (in cm^{-1}) of D, G and 2D bands and I_D/I_G ratio for pristine HOPG, HOPG–WPA (1:1) and HOPG–WPA (1:10)

Sample	D band	G band	2D band	I_D/I_G
pristine HOPG	1350	1581	2700	0.06
HOPG–WPA (1:1)	1350	1581	2700	0.08
HOPG–WPA (1:10)	1350	1581	2700	0.05

AFM was used to investigate the surface morphology of HOPG before and after treatment with WPA, at different acid concentrations. AFM images of pristine HOPG, HOPG–WPA (1:1) and HOPG–WPA (1:10) samples are shown in Fig. 2. For pristine HOPG, a wavy, grainy surface (Fig. 2a) can be seen with a measured surface roughness (RMS) of 35.0 nm. After treatment with the low concentration acid solution, a similar structure can be observed: wavy surface covered by grains. Considering the similarity between surface of HOPG and HOPG–WPA (1:1), the grains could not be ascribed to WPA, but they rather stem from HOPG itself. The value of RMS was calculated to be 35.8 nm. This result is in agreement with I_D/I_G ratio calculated from Raman spectra, which showed an increased structural disorder for the HOPG–WPA (1:1) sample. As for HOPG–WPA (1:10) sample, the AFM imaging indicated a slightly wavier surface (Fig. 2c). The calculated value of RMS was 29.6 nm. Again, the Raman measurements for the HOPG–WPA (1:10) sample indicated a less disordered structure, which resulted in the lower surface roughness.

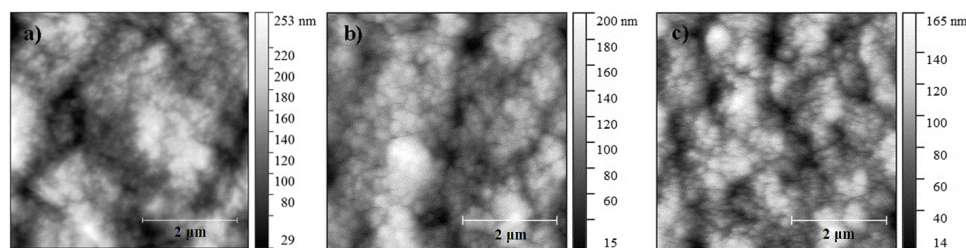


Fig. 2. Top-view AFM images of pristine HOPG (a), HOPG–WPA (1:1) (b) and HOPG–WPA (1:10) (c).

The Raman spectrum of pristine HOPG is compared with the spectra obtained for HOPG–MoPA samples with different mass ratios in Fig. S-2 (Supplementary material). The results of the spectral analysis are presented in Table III. While the Raman spectra of the HOPG–WPA samples did not show changes in the D, G and 2D band positions, the Raman spectra of the HOPG–MoPA samples displayed certain differences. The bands that stem from MoPA are again missing, and only the bands assigned to HOPG are present: D, G and 2D. The obtained results again indicated that there was no charge transfer between HOPG and MoPA.

TABLE III. Positions (in cm^{-1}) of D, G and 2D bands and I_D/I_G ratio for pristine HOPG, HOPG–MoPA (1:1) and HOPG–MoPA (1:10)

Sample	D band	G band	2D band	I_D/I_G
Pristine HOPG	1350	1581	2700	0.06
HOPG–MoPA (1:1)	1348	1582	2702	0.08
HOPG–MoPA (1:10)	1351	1582	2701	0.09

The I_D/I_G ratios of the HOPG–MoPA samples differed from the ratio for pristine HOPG, but in a different way compared to the HOPG–WPA samples. The trend of growth in the I_D/I_G ratio of the HOPG–MoPA samples followed the mass fraction of MoPA in the samples: the I_D/I_G intensity ratio had a higher value for sample with more MoPA. Therefore, a higher disorder was observed with increasing MoPA concentration.

AFM images of pristine HOPG, HOPG–MoPA (1:1) and HOPG–MoPA (1:10) are shown in Fig. 3. As can be seen, the observed surface morphology was similar for both the HOPG–MoPA (1:1) and HOPG–MoPA (1:10) samples. No MoPA clusters could be observed on either HOPG–MoPA samples. The calculation of surface roughness showed that for HOPG–MoPA (1:1), the *RMS* is 41.5 nm while for HOPG–MoPA (1:10), the *RMS* value is 47.6 nm. Compared to *RMS* value for pristine HOPG (35.0 nm), HOPG–MoPA (1:1) and HOPG–MoPA (1:10) showed significantly higher surface roughness. The *RMS* values increases with mass fraction of MoPA. These results confirm the higher disorder of HOPG observed by Raman spectroscopy.

Based on the presented results, it is evident that different amounts of acid had a different impact on HOPG. For this reason, the structural changes in HOPG when the HPAs were present in an excess were investigated.

The Raman spectra of pristine HOPG, HOPG–WPA (1:10)-C and WPA are shown in Fig. 4. Slight changes in the positions of the bands corresponding to HOPG are present in all the spectra.

While the shapes remained the same, the I_D/I_G ratio was changed from 0.06 (calculated for pristine HOPG) to 0.07 for the HOPG–WPA (1:10)-C sample. If these I_D/I_G values are compared with those obtained for the HOPG–WPA

samples (Table I), the opposite trend could be observed, *i.e.*, with the increase in the quantity of WPA the I_D/I_G ratio decreased. On the other hand, the band at 989 cm^{-1} , consisting of $\nu_{\text{as}}(\text{W}=\text{O}_d)$ and $\nu_{\text{s}}(\text{P}-\text{O}_a)$ stretching vibrations, loses its shape and upshifts by 3 cm^{-1} . These changes in Raman spectrum of WPA indicate the dehydration process of the acid due to laser heating.^{33,34} There is a change in intensity ratio of two prominent bands, at 1005 and 989 cm^{-1} , from 2.68 for WPA to 1.65 for HOPG–WPA (1:10)-C. However, it could be noticed that the Keggin structure was preserved, as the two main bands were present at 1006 and 992 cm^{-1} .

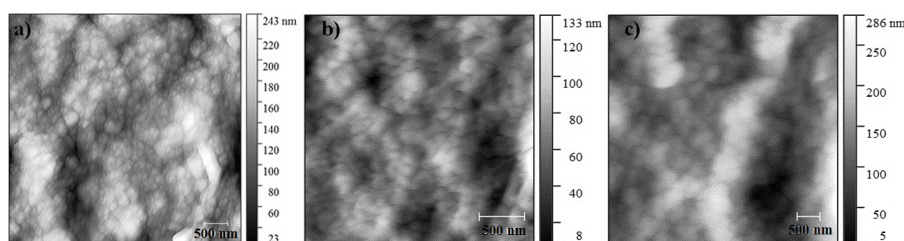


Fig. 3. Top view AFM images of pristine HOPG (a), HOPG–MoPA (1:1) (b) and HOPG–MoPA (1:10) (c).

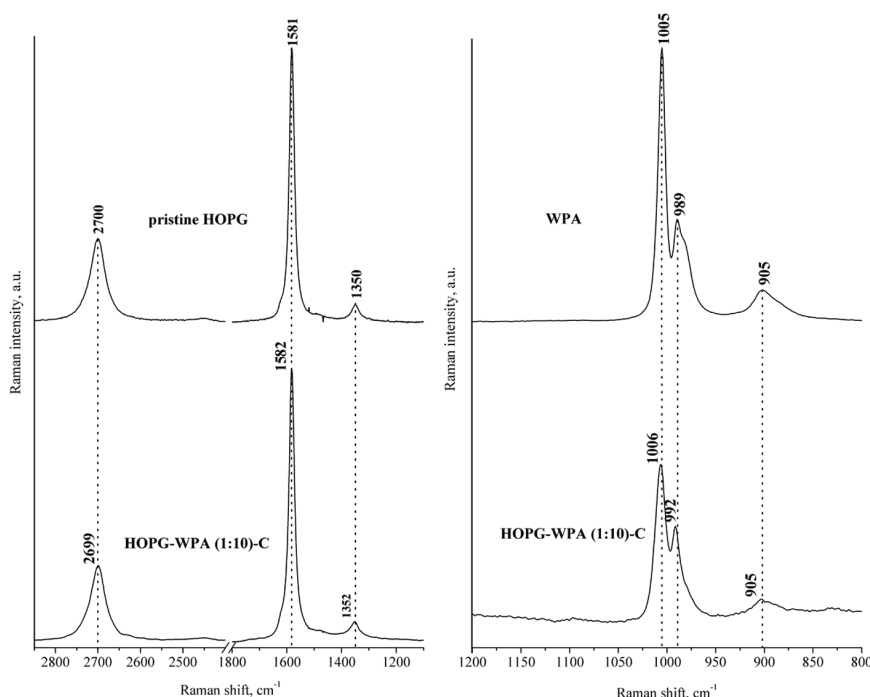


Fig. 4. Raman spectra of pristine HOPG and the HOPG–WPA-C sample in two different intervals.

Some changes in Raman spectra of the HOPG–MoPA (1:10)-C samples (unwashed and washed) could be observed (Fig. S-3, Supplementary material). The obtained band positions and intensity ratios I_D/I_G are listed in Table IV.

TABLE IV. Positions (in cm^{-1}) of the D, G and 2D bands and I_D/I_G ratio for pristine HOPG and HOPG–MoPA (1:10)-C samples

Sample	D band	G band	2D band	I_D/I_G
Pristine HOPG	1350	1581	2700	0.06
HOPG–MoPA (1:10)-C	1349	1581	2700	0.08
HOPG–MoPA (1:10)-C _W	1350	1579	2699	0.07

The most significant change was registered in the Raman spectrum of HOPG–MoPA (1:10)-C_W, where the position of the G band was downshifted by 2 cm^{-1} . The blue shift in the G band position is the result of a weak doping.³⁵ As could be noticed, the I_D/I_G ratio was slightly higher when MoPA was present in excess, in both HOPG–MoPA samples. Larger amounts of MoPA lead to the formation of a more defective structure, while this was not the case with WPA. Considering all these results, it could be concluded that MoPA has a much greater impact to the surface of HOPG than WPA.

The Raman spectra of MoPA and HOPG–MoPA (1:10)-C in the interval $1200\text{--}800 \text{ cm}^{-1}$ is shown in Fig. S-4 of the Supplementary material.

The positions of characteristic bands are presented in Table V. These results show significant downshifts of the band which stems from $\nu_s(\text{Mo}=\text{O}_d)$ vibration by 7 and 10 cm^{-1} for HOPG–MoPA (1:10)-C and HOPG–MoPA (1:10)-C_W, respectively. Based on the changes in the band positions, changes in the MoPA structure could be explained because of its interaction with the HOPG support. It is well known that Keggin anions in HPAs are stabilized mostly by dioxonium ions, but also by oxonium ions and protonated water.^{36–38} External oxygens interact with the support through oxonium ions (H_3O^+) and/or dioxonium ions (H_5O_2^+) of MoPA, causing prolongation and weakening of Mo–O bonds and a downshift of the $\text{Mo}=\text{O}_d$ band in the spectra.^{33,39}

TABLE V. Positions (in cm^{-1}) of characteristic bands in Raman spectra given in Fig. S-4

Sample	$\nu_s(\text{Mo}=\text{O}_d)$	$\nu_{as}(\text{Mo}=\text{O}_d)^a$
MoPA	993	971
HOPG–MoPA (1:10)-C	986	971
HOPG–MoPA (1:10)-C _W	983	966

^aComplex band consisting of $\nu_{as}(\text{W}=\text{O}_d)$ and $\nu_s(\text{P}=\text{O}_a)$

The Keggin anion of MoPA creates interaction with HOPG over the external oxygen atoms and caused weak doping of HOPG surface, which was a conclusion based on results presented in Table IV. These interactions caused a slight distortion of the MoPA anion and a downshifting of the $\nu_s(\text{Mo}=\text{O}_d)$ band for

HOPG–MoPA (1:10)-C and HOPG–MoPA (1:10)-C_W (Table V). Hence the downshifts and decrease in the intensity ratio of $\nu_s(\text{Mo}=\text{O}_d)$ and a mixture of the $\nu_{as}(\text{Mo}=\text{O}_d)$ and $\nu_s(\text{P}-\text{O}_a)$ vibrations indicate that the Keggin structure was preserved but slightly distorted.

In the literature, authors describe that interaction of HOPG and HPAs is realized by physical adsorption mainly because of the absence of the oxygen functional groups over HOPG surface. However, the basal surface of HOPG possess very low (electro)activity. Therefore we propose that HOPG sites located on the step edges intersecting the basal surface provide available sites for some interaction with MoPA, such as hydrogen bonding or charge transfer.⁴⁰

CONCLUSIONS

In this study, the interactions between HOPG and WPA or MoPA were observed using Raman spectroscopy and atomic force microscopy. Detailed analysis of used characterization techniques showed the following: there is no charge transfer between polyoxometalates and HOPG. Therefore, HOPG is not functionalized by these two heteropoly acids. Furthermore, there is only physisorption of molecules of the heteropoly acids on the HOPG surface. One of the major reasons for this is the absence of oxygen functional groups on the HOPG surface. Variations in the *RMS* and I_D/I_G ratio are strongly correlated and indicate the formation of defect structures on the HOPG surface. Based on these two parameters, it was established that the used heteropoly acids act differently on HOPG. It was found that HOPG interacts with MoPA and its Keggin anion creates interaction *via* the external oxygen atoms thereby causing weak doping of the HOPG surface. Comparing the values of the Raman shifts, HOPG formed stronger interactions with MoPA than with WPA.

Acknowledgements. The authors thank the Ministry of Education, Science and Technological Development of Republic of Serbia for financial support through national projects: Project Nos. 172003 and 172043.

ИЗВОД

ИСПИТИВАЊЕ ИНТЕРАКЦИЈА НОРГ И ПОЛИОКСОМЕТАЛАТА РАМАНСКОМ СПЕКТРОСКОПИЈОМ: ЕФЕКТИ РАЗЛИЧИТИХ КОНЦЕНТРАЦИЈА КИСЕЛИНА

БОЈАН А. ВИДОЕСКИ¹, СВЕТЛАНА П. ЈОВАНОВИЋ², ИВАНКА Д. ХОЛЦЛАЈТНЕР-АНТУНОВИЋ¹,
ДАНИЦА В. БАЈУК-БОГДАНОВИЋ¹, МИЛИЦА Д. БУДИМИР², ЗОРАН М. МАРКОВИЋ^{2,3}
и БИЉАНА М. ТОДОРОВИЋ МАРКОВИЋ²

¹Факултет за физичку хемију, б. бр. 47, Универзитет у Београду, 11158 Београд, ²Институт за нуклеарне науке „Винча“, б. бр. 522, Универзитет у Београду, 11001 Београд и ³Polymer Institute Slovak Academy of Sciences, Dubravska Cesta 9, Bratislava, Slovakia

Хетерополи киселине (HPAs) имају широку примену у катализи, складиштењу енергије, аналитичкој хемији, клиничкој медицини, науци о материјалима и другим областима, мада је због њихове мале слободне површине и високе растворљивости у води њихова примена ограничена. Један од приступа у решавању ових проблема је

коришћене материјала који имају велику слободну површину и могу се користити као њихови носачи, као на пример угљенични наноматеријали. Раманска спектроскопија је коришћена за испитивање интеракција између НРАs и високо-уређеног пиролитичког графита (НОРГ), одабраног као модела носача. Одабране су две киселине, 12-волфрам-фосфорна киселина и 12-молибден-фосфорна киселина којма је третирана површина НОРГ, у различитим концентрацијама. Примећено је да 12-молибден-фосфорна киселина има већи утицај на структуру НОРГ узрокујући слабо допирање и пораст структурне неуређености. Претпостављено је да НОРГ ступа у интеракцију са спољашњим атомима кисеоника 12-молибденфосфорне киселине. Микроскопом атомских сила утврђено је да се хрпаваост површине НОРГ третираног са 12-молибден-фосфорном киселином расте са порастом концентрације киселине, док у случају 12-волфрам-фосфорне киселине хрпаваост површине не зависи од њене концентрације. Пораст хрпавости површине НОРГ је у сагласности са променама структурне неуређеност (однос I_D/I_G) израчунатих на основу раманских спектра узорака НОРГ третираног са 12-молибден-фосфорном киселином.

(Примљено 1. марта, прихваћено 4. априла 2016)

REFERENCES

1. M. T. Pope, *Heteropoly and Isopoly Oxometalates*, Springer-Verlag, Berlin, 1983
2. M. T. Pope, A. Müller, *Polyoxometalate Chemistry From Topology via Self-Assembly to Applications*, Kluwer Academic Publishing, New York, 2001
3. J. M. Poblet, X. López, C. Bo, *Chem. Soc. Rev.* **32** (2003) 297
4. S. Liu, Z. Tang, *Nano Today* **5** (2010) 267
5. M. Fournier, R. Thouvenot, C. Rocchiccioli-Deltcheff, *J. Chem. Soc. Faraday Trans.* **87** (1991) 349
6. I. V. Kozhevnikov, *Chem. Rev.* **98** (1998) 171
7. R. T. Carr, M. Neurock, E. Iglesia, *J. Catal.* **278** (2011) 78
8. D. E. Katsoulis, *Chem. Rev.* **98** (1998) 359
9. C. L. Hill, *Chem. Rev.* **98** (1998) 1
10. S. Wang, H. Li, S. Li, F. Liu, D. Wu, X. Feng, L. Wu, *Chemistry* **19** (2013) 10895
11. P.-Y. Hoo, A. Z. Abdullah, *Chem. Eng. J.* **250** (2014) 274
12. N. H. H. Phuc, H. Ohkita, T. Mizushima, N. Kakuta, *Spectrochim. Acta., A* **99** (2012) 248
13. A. E. R. S. Khder, H. M. A. Hassan, M. S. El-Shall, *Appl. Catal., A* **411–412** (2012) 77
14. C. J. Boxley, H. S. White, T. E. Lister, P. J. Pinhero, *J. Phys. Chem., B* **107** (2003) 451
15. Y. Surendranath, D. A. Lutterman, Y. Liu, D. G. Nocera, *J. Am. Chem. Soc.* **134** (2012) 6326
16. F. Hui, J.-M. Noël, P. Poizot, P. Hapiot, J. Simonet, *Langmuir* **27** (2011) 5119
17. I. K. Song, M. S. Kaba, G. Coulston, K. Kourtakis, M. A. Barteau, *Chem. Mater.* **8** (1996) 2352
18. I. Song, *Catal. Today* **44** (1998) 285
19. M. S. Kaba, I. K. Song, D. C. Duncan, C. L. Hill, M. A. Barteau, *Inorg. Chem.* **37** (1998) 398
20. M. S. Kaba, M. A. Barteau, W. Y. Lee, I. K. Song, *Appl. Catal., A* **194** (2000) 129
21. I. K. Song, R. B. Shnitzer, J. J. Cowan, C. L. Hill, M. A. Barteau, *Inorg. Chem.* **41** (2002) 1292
22. I. K. Song, M. A. Barteau, *J. Mol. Catal. A Chem.* **182–183** (2002) 185
23. M. Rivera, S. Holguin, A. Moreno, J. D. Sepúlveda-Sánchez, T. Hernández-Pérez, *J. Electrochem. Soc.* **149** (2002) E84

24. I. K. Song, M. A. Barteau, *Korean J. Chem. Eng.* **19** (2002) 567
25. T. Hernández-Pérez, S. Holguín, M. Rivera, *J. Appl. Electrochem.* **34** (2004) 601
26. S.-H. Choi, J.-W. Kim, *Bull. Korean Chem. Soc.* **30** (2009) 810
27. G. Brauer, *Handbuch der Preparativen Anorganischen Chemie*, Ferdinand Enke Verlag, Stuttgart, 1981
28. I. Holclajtner-Antunović, D. Bajuk-Bogdanović, A. Popa, S. Uskoković-Marković, *Inorg. Chim. Acta* **383** (2012) 26
29. B. Todorović-Marković, S. Jovanović, V. Jokanović, Z. Nedić, M. Dramićanin, Z. Marković, *Appl. Surf. Sci.* **255** (2008) 3283
30. Gwyddion, <http://www.gwyddion.net> (accessed February 15th, 2016)
31. M. S. Dresselhaus, A. Jorio, A. G. Souza Filho, R. Saito, *Philos. Trans. R. Soc., A: Math. Phys. Eng. Sci.* **368** (2010) 5355
32. A. C. Ferrari, *Solid State Commun.* **143** (2007) 47
33. C. Rocchiccioli-Deltcheff, M. Fournier, R. Franck, R. Thouvenot, *Inorg. Chem.* **22** (1983) 207
34. F. D. Hardcastle, I. E. Wachs, *J. Raman Spectrosc.* **21** (1990) 683
35. A. Jorio, M. S. Dresselhaus, R. Saito, G. Dresselhaus, *Raman Spectroscopy in Graphene Related Systems*, Wiley-VCH Verlag, New York, 2011
36. H. Ratajczak, A. J. Barnes, A. Bielański, H. D. Lutz, A. Müller, in: *Polyoxometalate Chemistry From Topology via Self-Assembly to Applications*, A. Müller, M. T. Pope, Eds., Springer, Amsterdam, 2001, p. 101
37. U. Mioč, M. R. Todorović, M. Davidović, Ph. Colomban, I. Holclajtner-Antunović, *Solid State Ionics* **176** (2005) 3005
38. U. B. Mioč, M. Petković, M. Davidović, M. Perić, T. Abdul-Redah, *J. Mol. Struct.* **885** (2008) 131
39. S. Damyanova, L. M. Gomez, M. A. Bañares, J. L. G. Fierro, *Chem. Mater.* **12** (2000) 501
40. C.-Y. Lee, A. M. Bond, *Anal. Chem.* **81** (2009) 584.